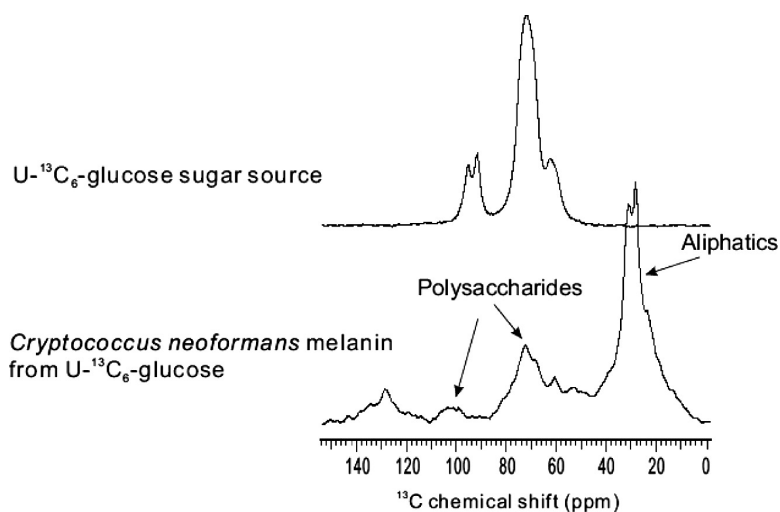


## Following Fungal Melanin Biosynthesis with Solid-State NMR: Biopolymer Molecular Structures and Possible Connections to Cell-Wall Polysaccharides

Junyan Zhong, Susana Frases, Hsin Wang, Arturo Casadevall, and Ruth E. Stark

*Biochemistry*, 2008, 47 (16), 4701-4710 • DOI: 10.1021/bi702093r • Publication Date (Web): 28 March 2008

Downloaded from <http://pubs.acs.org> on May 7, 2009



### More About This Article

Additional resources and features associated with this article are available within the HTML version:

- Supporting Information
- Access to high resolution figures
- Links to articles and content related to this article
- Copyright permission to reproduce figures and/or text from this article

[View the Full Text HTML](#)



ACS Publications  
High quality. High impact.

# Following Fungal Melanin Biosynthesis with Solid-State NMR: Biopolymer Molecular Structures and Possible Connections to Cell-Wall Polysaccharides<sup>†</sup>

Junyan Zhong,<sup>‡</sup> Susana Frases,<sup>§</sup> Hsin Wang,<sup>‡,||</sup> Arturo Casadevall,<sup>§</sup> and Ruth E. Stark<sup>\*,‡,||</sup>

Departments of Chemistry, College of Staten Island and City College of New York, City University of New York Graduate Center and Institute for Macromolecular Assemblies, New York, New York 10031–9101, and Department of Microbiology & Immunology, Albert Einstein College of Medicine, Yeshiva University, Bronx, New York 10461-1900

Received October 17, 2007; Revised Manuscript Received February 8, 2008

**ABSTRACT:** Melanins serve a variety of protective functions in plants and animals, but in fungi such as *Cryptococcus neoformans* they are also associated with virulence. A recently developed solid-state nuclear magnetic resonance (NMR) strategy, based on the incorporation of site-specific <sup>13</sup>C-enriched precursors into melanin, followed by spectroscopy of both powdered and solvent-swelled melanin ghosts, was used to provide new molecular-level insights into fungal melanin biosynthesis. The side chain of an L-dopa precursor was shown to cyclize and form a proposed indole structure in *C. neoformans* melanin, and modification of the aromatic rings revealed possible patterns of polymer chain elongation and cross-linking within the biopolymer. Mannose supplied in the growth medium was retained as a β-pyranose moiety in the melanin ghosts even after exhaustive degradative and dialysis treatments, suggesting the possibility of tight binding or covalent incorporation of the pigment into the polysaccharide fungal cell walls. In contrast, glucose was scrambled metabolically and incorporated into both polysaccharide cell walls and aliphatic chains present in the melanin ghosts, consistent with metabolic use as a cellular nutrient as well as covalent attachment to the pigment. The prominent aliphatic groups reported previously in several fungal melanins were identified as triglyceride structures that may have one or more sites of chain unsaturation. These results establish that fungal melanin contains chemical components derived from sources other than L-dopa polymerization and suggest that covalent linkages between L-dopa-derived products and polysaccharide components may serve to attach this pigment to cell wall structures.

The natural melanin pigments of vertebrates, insects, plants, and microbial organisms serve important roles in camouflage, in sexual display, and for protection against solar radiation (1). Yet from a biomedical standpoint their association with living cells can also be detrimental: a melanin has been implicated in neurodegenerative diseases (2), the pigment is thought to account for the resistance of human melanoma tumors to radiative and chemical therapies (3, 4), and melanization may be responsible for virulence in several pathogenic fungi that strike immunocompromised individuals

(5). Although these materials have been proposed to be phenol- or indole-based polymers based on degradation studies (6), intact melanins have proven challenging to characterize at the molecular level. Historically, their insolubility has precluded traditional spectroscopic or hydrodynamic examination, and their amorphous character has prevented structure determination by X-ray crystallography.

Previously, solid-state nuclear magnetic resonance (NMR<sup>1</sup>) methods were used to establish the major carbon- and nitrogen-containing functional groups in eumelanins from animal and fungal sources (7–11). More recently, Bowers and co-workers reported CPMAS results for *Sepia officinalis* and *Human hair* melanin along with crystalline model compounds (2), identifying a variety of indole, pyrrole, carbonyl, and protein-derived aliphatic functional groups. Concurrently, our group applied solid-state NMR techniques to both powdered and solvent-swelled *Cryptococcus neoformans* melanin ghosts (12). This latter work established that melanin has a substantial aliphatic character and identified several functional groups using their through-bond spin connectivities. Furthermore, we demonstrated the feasibility

<sup>†</sup> This work was supported by a grant from the National Institutes of Health (AI052733). The 300 and 600 MHz NMR spectrometers were supported by the College of Staten Island and the CUNY Institute for Macromolecular Assemblies, a Center of Excellence of the Generating Employment through New York State Science program. The 750 MHz NMR spectrometer was supported by NIH P41 GM66354 to the New York Structural Biology Center (NYSBC). R.E.S. is a member of the NYSBC, a STAR center supported by the New York State Office of Science, Technology, and Academic Research.

\* To whom correspondence should be addressed. E-mail: stark@sci.cny.cuny.edu. Phone: 212-650-8916. Fax: 212-650-8719. CUNY Institute for Macromolecular Assemblies, The City College of New York, Department of Chemistry, 138th Street and Convent Avenue, New York, NY 10031-9101.

<sup>‡</sup> Department of Chemistry, College of Staten Island, City University of New York Graduate Center and Institute for Macromolecular Assemblies.

<sup>§</sup> Yeshiva University.

<sup>||</sup> Department of Chemistry, City College of New York, City University of New York Graduate Center and Institute for Macromolecular Assemblies.

<sup>1</sup> Abbreviations: L-dopa, L-3,4-dihydroxyphenylalanine; NMR, nuclear magnetic resonance; CPMAS, cross-polarization magic-angle spinning; HRMAS, high-resolution magic-angle spinning; PBS, phosphate-buffered saline; gHMQC, <sup>1</sup>H–<sup>13</sup>C gradient-assisted heteronuclear multiple-quantum coherence; gmqCOSY, multiple-quantum filtered correlated spectroscopy; gHMQC-TOCSY, gHMQC-total correlation spectroscopy; gHMBC, <sup>1</sup>H–<sup>13</sup>C gradient-assisted heteronuclear multiple-bond correlation.

of studying melanin structure through the incorporation of exogenous precursors with  $^{13}\text{C}$  labels into aromatic portions of the biopolymer structure (12). Thus a novel NMR approach was developed to unlock the molecular structure of melanin, paving the way for studies of its biosynthesis and the onset of fungal pathogenicity.

Melanization in *C. neoformans* involves the synthesis of melanin granules in the cell wall. However, the mechanism by which such granules are assembled and held in place is unknown (13). Understanding the mechanisms of melanin synthesis can have implications in various fields including the development of new antimicrobial drugs, cancer therapy and energy transduction. Interference with melanization produces a therapeutic effect in mice with experimental cryptococcal infection, suggesting that drugs that target the melanin synthesis and cellular assembly pathways may be potential antimicrobial agents for melanotic microorganisms (reviewed in ref 14). The similarities between cryptococcal and mammalian melanin have been exploited to develop monoclonal antibodies that are in clinical evaluation for the treatment of melanoma (reviewed in ref 15). Finally, there are tantalizing indications that melanin can function in energy transduction, allowing melanotic microbes to capture high energy ionizing radiation (16).

In the current investigation, NMR methods were used to monitor the indole formation that is proposed to occur in *C. neoformans* via the Mason–Raper pathway for melanin biosynthesis (17, 18), to investigate the source and molecular identity of aliphatic moieties associated with the pigment from this fungus, and to address the issue of whether the polysaccharide fungal cell wall is tightly associated or covalently bound to the melanin biopolymer. Because *C. neoformans* requires exogenous precursors for melanization, it was possible to follow the metabolic transformations by growing the cells in the presence of a selection of  $^{13}\text{C}$ -enriched L-dopa precursors and sugar sources: single  $^{13}\text{C}$  labels ( $1\text{-}^{13}\text{C}\text{-D-mannose}$ ),  $^{13}\text{C}\text{-}^{13}\text{C}$  pairs ( $2,3\text{-}^{13}\text{C}\text{-L-dopa}$ ), and more extensively labeled materials (ring- $^{13}\text{C}_6\text{-L-dopa}$  and  $\text{U-}^{13}\text{C}_6\text{-glucose}$ ). Our results provide evidence for L-dopa-derived indole formation and the incorporation of carbohydrate and triglyceride compounds into this fungal melanin.

## MATERIALS AND METHODS

*C. neoformans* Melanin “Ghosts”. *C. neoformans* strain 24067 was obtained from the American Tissue Type Collection (Rockville, MD) and grown as described previously (19), by shaking at 30 °C for two weeks in minimal media (29.4 mM  $\text{KH}_2\text{PO}_4$ , 10 mM  $\text{MgSO}_4 \cdot 7\text{H}_2\text{O}$ , 13 mM glycine, 15 mM D-glucose, and 3  $\mu\text{M}$  thiamine) supplemented with 1 mM L-dopa (Sigma Chemical, St. Louis, MO) and then suspended in phosphate-buffered saline (PBS). The cells were collected by centrifugation at 1370g (Sorvall SLA-1500, Sorvall RC5Cplus, Kendro, GMI, Inc., Minnesota) for 10 min and suspended in a 1.0 M sorbitol/0.1 M sodium citrate solution at pH 5.5. Protoplasts were generated by overnight incubation at 30 °C in 10 mg/ml of cell wall-lysing enzymes (*Trichoderma harzianum*, Sigma Chemical Co, St. Louis, MO). The protoplasts were collected by centrifugation, washed with PBS, and incubated in 4.0 M guanidine thiocyanate for 12 h at room temperature with frequent vortexing. The resulting black material was collected by

centrifugation and washed with PBS, then treated with 1.0 mg/ml Proteinase K (Roche Molecular Biochemicals, Indianapolis, IN) to separate residual proteins from the cell walls. The particles were then washed three times with PBS, extracted with a 1:1 (v/v) phenol–chloroform mixture, and boiled in 6.0 M HCl for one hour to hydrolyze cellular contaminants associated with melanin. The black particles of interest were collected by centrifugation, washed with water, and dialyzed for two weeks with daily water changes. The total carbohydrate concentration of the supernatant from the resulting suspension was 0.097 mg/112 mg ghosts, as determined by a phenol–sulfuric acid assay (20). The typical elemental composition (C:N:O) for the black particles is 29:2:6 (19).

In selected experiments,  $2,3\text{-}^{13}\text{C}_2$ (97%),  $4\text{-}^{18}\text{OH}$  (95%)-L-dopa or ring- $^{13}\text{C}_6\text{-L-dopa}$  was used as melanin precursors; in other experiments 1:1 (mol/mol)  $1\text{-}^{13}\text{C}$ (99%)-D-mannose: D-glucose or  $\text{U-}^{13}\text{C}$ (99%)-glucose was used as sugar source (all isotopically enriched materials from Cambridge Isotope Laboratories, Andover, MA).

*Magnetic Resonance Experiments.* Solid-state NMR experiments for the black melanin particles were conducted on either of two spectrometers. At The College of Staten Island, a Varian (Palo Alto, CA) UNITYplus widebore spectrometer operating at a  $^{13}\text{C}$  frequency of 75.4 MHz was used. Unless noted otherwise, 10–30 mg powdered samples were examined using a 5 mm probe from Doty Scientific (Columbia, SC) spinning at  $9.00 \pm 0.01$  kHz and room temperature. At the New York Structural Biology Center, 15–25 mg samples were examined in a 4 mm probe using a Bruker (Billerica, MA) AVANCE widebore spectrometer operating at 188.7 MHz for  $^{13}\text{C}$  and with MAS at  $15.000 \pm 0.002$  kHz. Cross-polarization magic-angle spinning (CP-MAS)  $^{13}\text{C}$  experiments at 75 MHz were conducted with 1 ms 50 kHz  $^1\text{H}\text{-}^{13}\text{C}$  spin-lock contacts, a  $^1\text{H}$  decoupling strength of 75 kHz, and recycle times of 1–2 s between successive acquisitions. At 189 MHz, a 50 kHz  $^{13}\text{C}$  radio-frequency field was matched with a  $^1\text{H}$  field ramped from 40 to 80 kHz during a typical period of 1 ms, the TPPM method (21) was used for  $^1\text{H}$  decoupling, and the recycle time was 3 s. Exponential line broadening of 100 Hz was used to condition the spectra; chemical shifts were referenced to external hexamethylbenzene and quoted with respect to tetramethylsilane.

For swelled-solid experiments, data were acquired on a UNITYINOVA 600 NMR spectrometer operating at a  $^1\text{H}$  frequency of 599.944 MHz. Typically, 5 mg of melanin ghosts were equilibrated with 48 mg of  $\text{DMSO-}d_6$  at 50 °C in a 40  $\mu\text{L}$   $^1\text{H}$ -optimized nanoprobe equipped with 160 G/cm pulsed field gradients and spun at  $2.800 \pm 0.001$  kHz. HRMAS NMR included one-pulse spectral acquisitions and a variety of two-dimensional  $^1\text{H}\text{-}^{13}\text{C}$  gradient-assisted experiments: heteronuclear multiple-quantum coherence (gHMQC) (22), multiple-quantum filtered correlated spectroscopy (gmqCOSY) (23), gHMQC-TOCSY (24, 25), and heteronuclear multiple-bond correlation (gHMBC) (26) experiments with 11 G/cm gradients for coherence selection, implemented by synchronizing the gradient times with the rotor periods. Pulse sequence delays in the gHMQC and gHMBC experiments were optimized for one-bond and multiple-bond  $J$ -couplings of 150 and 8 Hz, respectively. Solvent suppression was done by presaturation of the residual

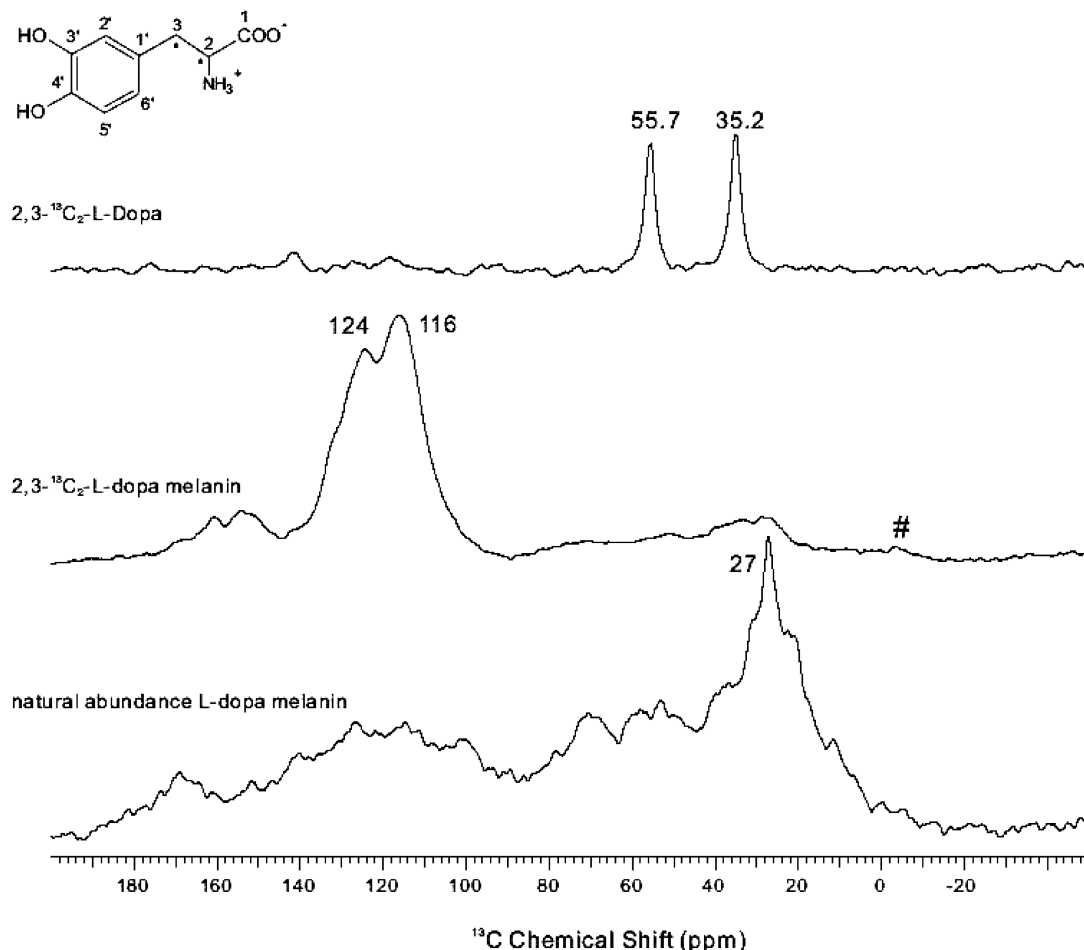


FIGURE 1: 75.4 MHz  $^{13}\text{C}$  CPMAS NMR spectra of  $2,3\text{-}^{13}\text{C}_2\text{-L-dopa}$  (top), the derived *C. neoformans* melanin ghosts (middle, 33,000 transients), and ghosts produced from natural abundance precursors (bottom, 57,000 transients). The 30 mg samples were spun at 9 kHz for the melanins (12) and 7 kHz for the precursor; data were acquired with 1 ms 50 kHz  $^1\text{H}\text{-}^{13}\text{C}$  spin-lock contacts and 75 kHz proton decoupling in each case. The (#) designation shows the position of a spinning sideband.

water resonance at 3.29 ppm. Typical experimental parameters included a recycle delay of 1 s;  $90^\circ$  pulse widths of 4.7  $\mu\text{s}$  for  $^1\text{H}$  and 9.2  $\mu\text{s}$  for  $^{13}\text{C}$ ; spectral widths of 6000 and 25,649 Hz for  $^1\text{H}$  and  $^{13}\text{C}$ , respectively. The GARP sequence (27) was used for  $^{13}\text{C}$  decoupling.  $^1\text{H}$  and  $^{13}\text{C}$  chemical shifts were referenced to DMSO at 2.49 and 39.5 ppm, respectively. The gHMQC-TOCSY experiments were conducted with adiabatic mixing (28).

Simulations of  $^{13}\text{C}$  NMR spectra were conducted with ACD carbon chemical shift predictor software (Advanced Chemistry Development Inc., Toronto, Canada). Electron paramagnetic resonance (EPR) experiments were carried out on a Bruker EMX spectrometer located at Hunter College.

## RESULTS AND DISCUSSION

**Conversion of the L-Dopa Side Chain to Indole Ring Structures.** In order to examine the metabolic fate of the obligatory L-dopa precursor, CPMAS  $^{13}\text{C}$  NMR spectra were compared for  $2,3\text{-}^{13}\text{C}_2\text{-L-dopa}$  and its corresponding *C. neoformans* melanin product (Figure 1). Whereas the isotopically enriched aliphatic carbons of the L-dopa (previously designated incorrectly as 2',3' positions on the aromatic ring (12)) resonate at 35.2 and 55.7 ppm, respectively, the predominant spectral features of the fungal melanin

correspond to aromatic residues at 116 and 124 ppm. Additional peaks at 154 and 161 ppm may be attributed to side products.

These changes in chemical shift suggest that the side chain of L-dopa forms a cyclic aromatic structure during melanin biosynthesis, consistent with the indole-based polymers proposed in the Mason–Raper scheme for *C. neoformans* biosynthesis (17). According to this hypothesis (Figure 2), the molecular architecture of the melanin pigment is expected to resemble that exemplified by the 5,6-indolequinone (IQ) or 5,6-dihydroxyindole (DHI) biosynthetic intermediates. Indeed, the 116 and 124 ppm  $^{13}\text{C}$  chemical shifts of L-dopa melanin are in good agreement with the 110 and 126 ppm reports for C-3 and C-2 of solid DHI (29). By contrast, the ACD spectral database software, which was validated for L-dopa, predicts a C-2 chemical shift of 142 ppm for IQ; this latter intermediate is also less likely to be present in our NMR spectra because of its thermodynamic instability (30).

The broad appearance of the aromatic spectral region could include contributions from free radicals, given the observation of EPR signals for this and related samples (available as Supporting Information 2, 31). The observation of a single symmetric EPR peak with no hyperfine structure argues against unpaired electron density localized near the  $^{14}\text{N}$  of

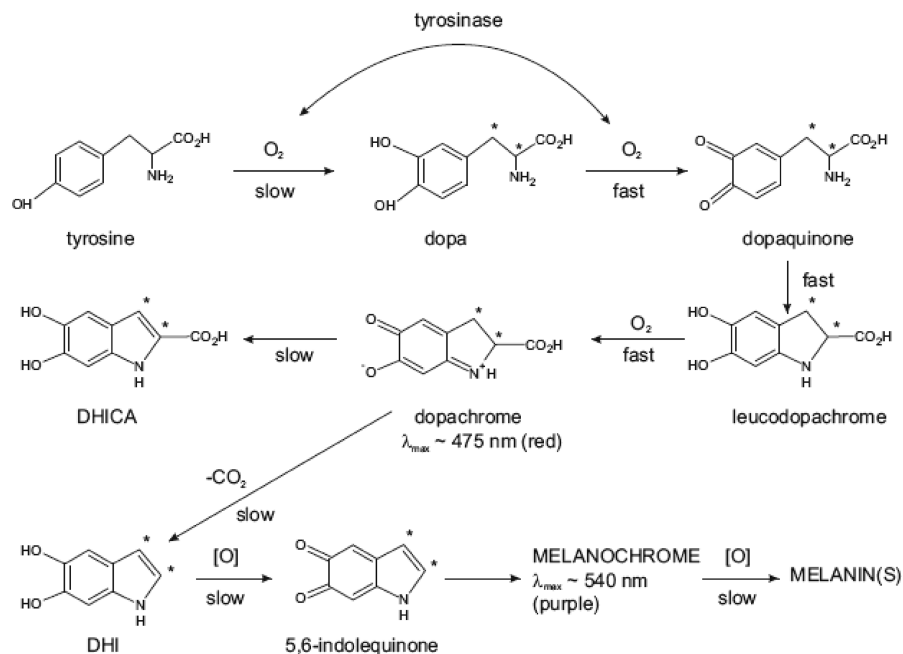


FIGURE 2: Mason–Raper scheme of melanogenesis. The early step in which tyrosinase catalyzes the conversion of tyrosine to L-dopa has been omitted. Asterisks are used to track the enriched carbons from a 2,3- $^{13}C_2$ -L-dopa precursor. Adapted from ref 17.

an indole ring and in favor of more generalized relaxation effects, if they are present. However, paramagnetic broadening need not be invoked because the melanin polymer is amorphous and the four overlapping resonances resolved in 2D  $^{13}C$ – $^{13}C$  spin diffusion experiments (12) will produce a broad envelope in the 1D NMR spectrum. These latter features could arise from a set of structurally similar melanins produced by the 2,3- $^{13}C_2$ -L-dopa precursor. Moreover, prior  $^1H$ -mediated  $^{13}C$ – $^{13}C$  spin diffusion measurements showed that roughly half of the isotopically enriched carbon pairs remain proximal (and probably covalently bound) in the melanin pigment (12), as anticipated from molecular structures proposed in the Mason–Raper scheme. Spectroscopic evidence for an indole ring has also been reported from CPMAS  $^{15}N$  NMR of diverse melanins (available as Supporting Information) (2, 8, 10).

**L-Dopa Phenolic Rings and Possible Polymeric Structures.** Additional information on the molecular structures derived from L-dopa came from experiments using ring- $^{13}C_6$ -L-dopa as a precursor in *C. neoformans* melanin biosynthesis. Figure 3 displays CPMAS  $^{13}C$  NMR spectra of the precursor and associated melanin product, demonstrating the basic aromatic ring structure in both materials. The spectrum of the material derived from the labeled precursor displays no significant carbonyl resonances near 178 ppm, arguing against a quinone structure; instead the substantial signal intensity at 143 ppm supports retention of a C-3',C-4' *ortho*-diphenol structure as judged from ACD modeling and prior literature (2, 29). Although broadened spectral features in the melanin may be indicative of a heterogeneous biopolymer or unpaired electron density as noted above, the resolution is sufficient to distinguish the aromatic and aliphatic carbon functionalities. For instance, the similarity of chemical shifts for C-3' and C-4' of the precursor and the product resonance centered at 143 ppm suggests that these sites are unchanged chemically. By contrast, C-1', C-2', C-5', and C-6' resonances (112–124 ppm) now appear at 94–124 ppm, implicating structural changes. The latter trends could be explained by

formation of a new indole ring spanning C-1' and C-6' and polymer chain elongation via C-2' and C-5'. The inset to Figure 3 shows proposed cross-linked and branched melanin chain structures (32) that are consistent with the observed  $^{13}C$  chemical shifts. As noted above, CPMAS  $^{15}N$  NMR also supports the presence of an indole ring in various melanins (2, 8, 10) (this work, available as Supporting Information). An enrichment factor in excess of 40-fold may be estimated by comparison of signal intensities (e.g., aromatics at 143 ppm or chain methylenes at 27 ppm) between the natural abundance and  $^{13}C$ -labeled samples, though any numerical estimate must be viewed as approximate due to spectral overlap between enriched and unenriched moieties and variability among nominally identical *C. neoformans* samples.

**Incorporation of Mannose into Melanizing *C. neoformans* Cells.** Although poor yields of *C. neoformans* melanin were obtained using mannose as the only sugar source, growth of the cells in the presence of natural-abundance L-dopa and a 1:1 mixture of glucose and 1- $^{13}C$ -D-mannose sugars gives the expected yield of melanin ghosts in which the isotopically enriched C-1 resonance appeared prominently at 101.5 ppm in the CPMAS  $^{13}C$  NMR spectrum (Figure 4). Metabolic scrambling to other carbon moieties, as judged from enhanced signal intensity in the mannose-enriched melanin NMR spectra, appeared to be minor. Given the exhaustive enzymatic and chemical treatments used to prepare the ghosts, the retention of a sugar-derived moiety raises the possibility that the indole-based pigment is bound covalently to the polysaccharide fungal cell wall. In contrast to the spectroscopic data obtained with 2,3- $^{13}C_2$ -L-dopa and ring- $^{13}C_6$ -L-dopa as melanin precursors, the  $^{13}C$ -labeled resonance originating from 1- $^{13}C$ -D-mannose did not dominate the CPMAS spectrum. Given the relatively modest signal intensity evident near 100 ppm in the natural-abundance L-dopa melanin spectrum, this result is reasonable. Since among the aliphatic resonances only the  $^{13}C$ -enriched C-1 sugar signal shows increased intensity, our hypothesis is that

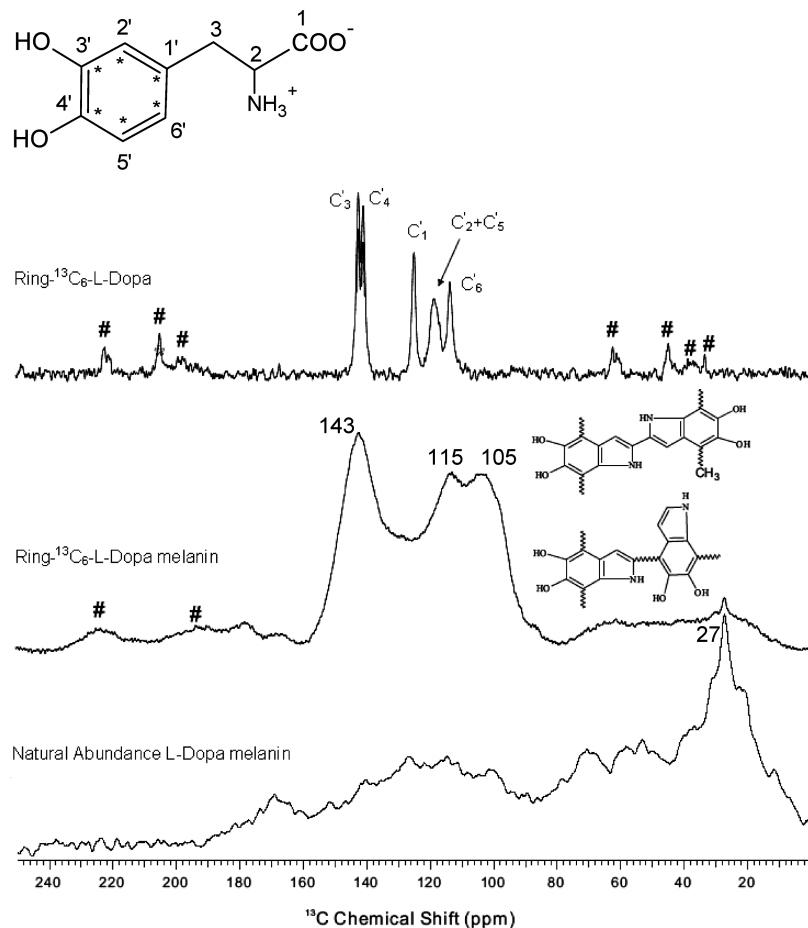


FIGURE 3: CPMAS  $^{13}\text{C}$  NMR spectra of ring- $^{13}\text{C}_6$ -L-dopa (top, 188.7 MHz), its derived *C. neoformans* melanin ghosts (middle, 15 mg, 256 transients, 188.7 MHz), and ghosts produced from natural abundance precursors (bottom, 30 mg, 57,000 transients, 75.4 MHz). The high-field data were obtained with 15 kHz MAS, and the low-field data were acquired with 9 kHz MAS. Positions of spinning sidebands are designated by (#). Resonance assignments for the L-dopa precursor and proposed melanin chain structures were taken from Adhyaru et al. (2).

the mannose was incorporated directly into the polysaccharide cell wall rather than being broken down before use as a nutrient for fungal growth.

To rule out the possibility of metabolic scrambling, HRMAS  $^1\text{H}$  NMR spectra were acquired for solvent-swelled melanin samples (Figure 5). As compared with previously published HRMAS spectra (12), improved swelling and acquisition protocols made it possible to observe greater spectral detail, though aromatic groups were still underrepresented. For the isotopically enriched mannose precursor, the H-1 proton displays a doublet that collapses upon  $^{13}\text{C}$  decoupling (Figure 5, inset). However, the spectra of the corresponding *C. neoformans* melanin were identical under the two acquisition conditions. Thus neither the abundant aliphatic nor sugar moieties become  $^{13}\text{C}$ -enriched by metabolic scrambling under these growth conditions.

As noted above, the less-than-dominant pigment NMR signal derived from 1- $^{13}\text{C}$ -D-mannose may simply reflect a modest relative number of glycosidic moieties retained in the melanin ghosts. The observation of a HRMAS-HMQC cross-peak at (101.8, 4.48 ppm) for DMSO-swelled 1- $^{13}\text{C}$ -D-mannose melanin (Figure 6) allowed us to suggest that the small resonance at 4.5 ppm in the HRMAS spectrum is H-1 (Figure 5). If the resonances at 3.88, 3.97, and 4.16 ppm are each taken to represent a glycerol-like melanin constituent (see below) and it is assumed that all  $\text{CH}_n\text{O}$  groups are

swelled by DMSO with comparable efficiency, then integration of the anomeric mannose proton resonance indicates that roughly 1 in every 10 melanin structures is associated with a mannose-derived sugar unit in the polysaccharide cell wall. In this latter scenario, it may be proposed that one anomer of the 1- $^{13}\text{C}$ -D-mannose supplied by the growth medium is incorporated directly into cell wall mannose containing polysaccharides as shown for glucuronoxylomannan (33), most of which are then hydrolyzed enzymatically and removed to leave only those sugar-derived structures at the interface with the melanin polymer in the ghost samples.

*Possible Covalent Bonding of C. neoformans Cell-Wall Polysaccharides to Melanin.* Additional evidence supporting the covalent bonding of mannose within melanin ghosts comes from  $^{13}\text{C}$  and  $^1\text{H}$  chemical shift trends. Figure 6 shows that the  $\text{C}_1$  carbons resonate at 101 and 102 ppm in the HRMAS-HMQC NMR spectrum of DMSO-swelled 1- $^{13}\text{C}$ -D-mannose melanin, implicating altered chemical environments compared with the corresponding  $\text{C}_1$  carbons of  $\alpha$ - and  $\beta$ -pyranose forms of the free D-mannose, which resonate at 93.6 and 93.8 ppm, respectively (34). Thus rather than residual free sugars, our spectroscopic results support the presence of a functionalized  $\beta$ -pyranose form of mannose. The values of chemical shift are consistent with either a polysaccharide or a sugar-melanin connection (35). The

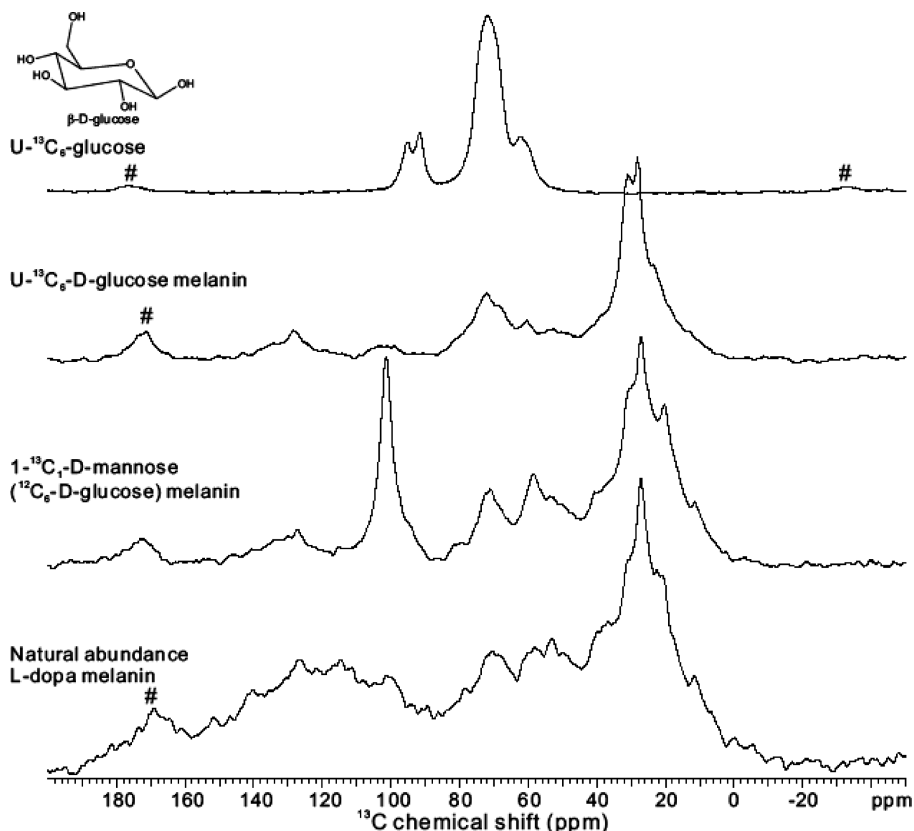


FIGURE 4: 75.4 MHz CPMAS NMR spectra of a sugar source and various *C. neoformans* melanin ghosts produced with a natural abundance L-dopa precursor. The data (shown from top to bottom) were obtained with spinning at 7.8, 10, 10 and 9 kHz, respectively and recycle times varying between 1 and 2 s. The  $^{13}\text{C}$  NMR spectrum of the  $1\text{-}^{13}\text{C}\text{-D-mannose}$  sugar (not shown) displays a prominent resonance at 95 ppm.

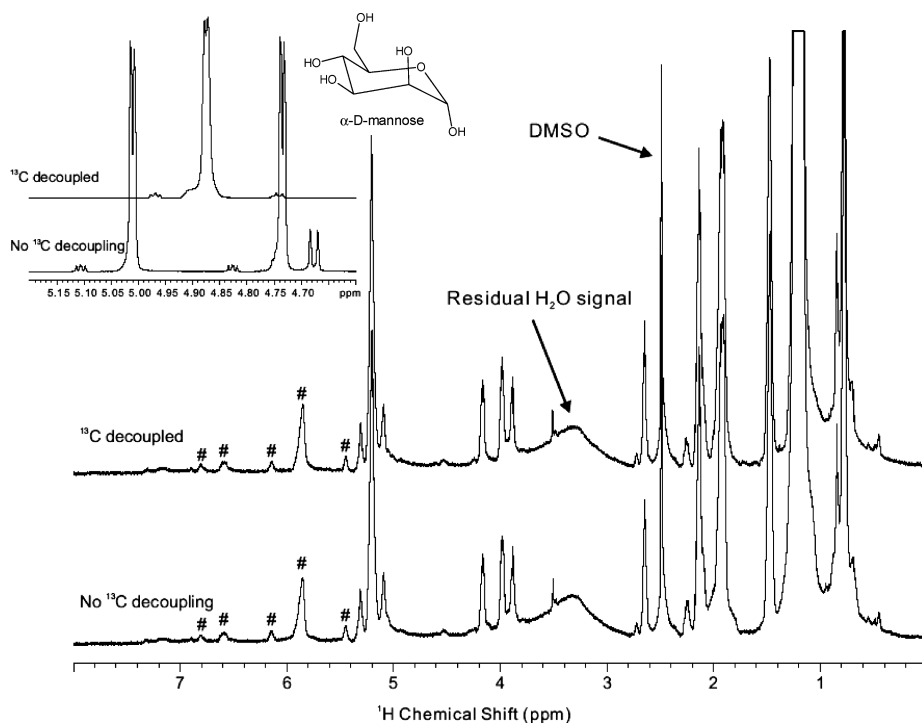


FIGURE 5: 600 MHz  $^1\text{H}$  HRMAS spectra of melanin ghosts derived from natural-abundance L-dopa and a 1:1 mixture of glucose and  $1\text{-}^{13}\text{C}\text{-}\alpha\text{-D-mannose}$ . The melanin sample was swollen in  $\text{DMSO-}d_6$  at  $50^\circ\text{C}$  and spun at 2.800 kHz. The inset shows solution-state spectra of the  $1\text{-}^{13}\text{C}\text{-}\alpha\text{-D-mannose}$  precursor, illustrating the effects of  $^{13}\text{C}$  decoupling. Signals in the downfield aromatic region are more prominent if the sample is ground (not shown).

latter explanation has precedent in prior observations of mannose-containing polysaccharide motifs in the *C. neoformans* cell wall, including galactoxylomannan (36) and

mannosylated proteins such as mannoproteins (37). These observations then raise the tantalizing possibility that melanin is anchored into the cell wall through a covalent linkage with

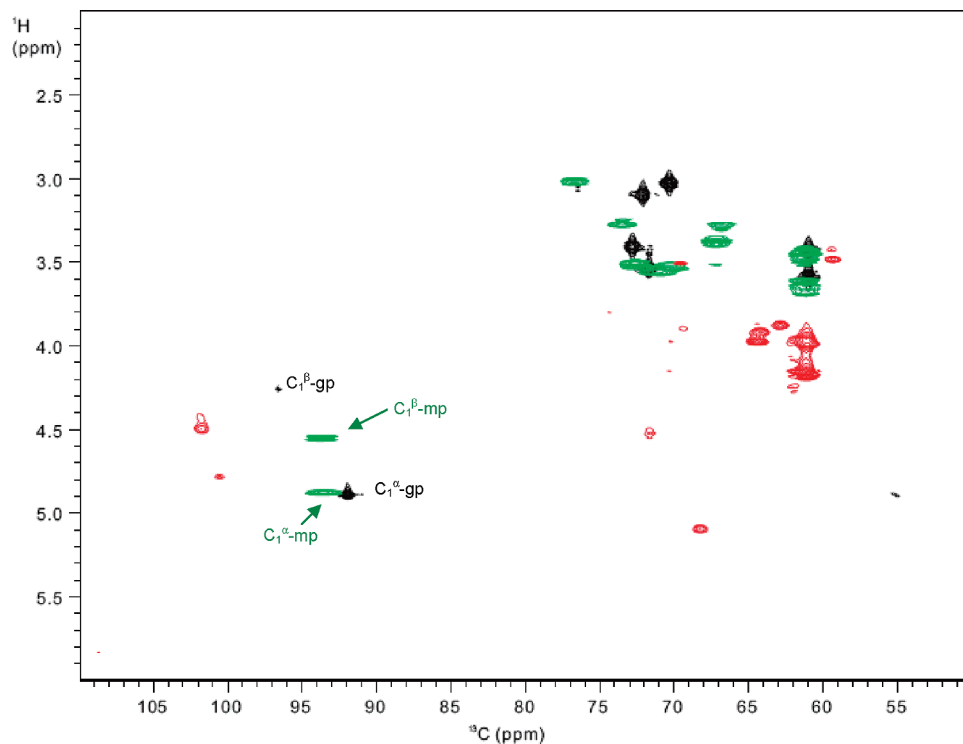


FIGURE 6: Superimposed 2D contour plots of the sugar and glyceride region in HRMAS-gHMQC spectra of D-glucose (black), D-mannose (green), and fungal melanin ghosts derived from L-dopa and a 1:1 glucose:1-<sup>13</sup>C-mannose mixture (red); mp, mannopyranose; gp, glucopyranose. The spectra were acquired at a proton Larmor frequency of 600 MHz. The spinning speed and sample temperature were  $2.800 \pm 0.001$  kHz and  $50$  °C, respectively.

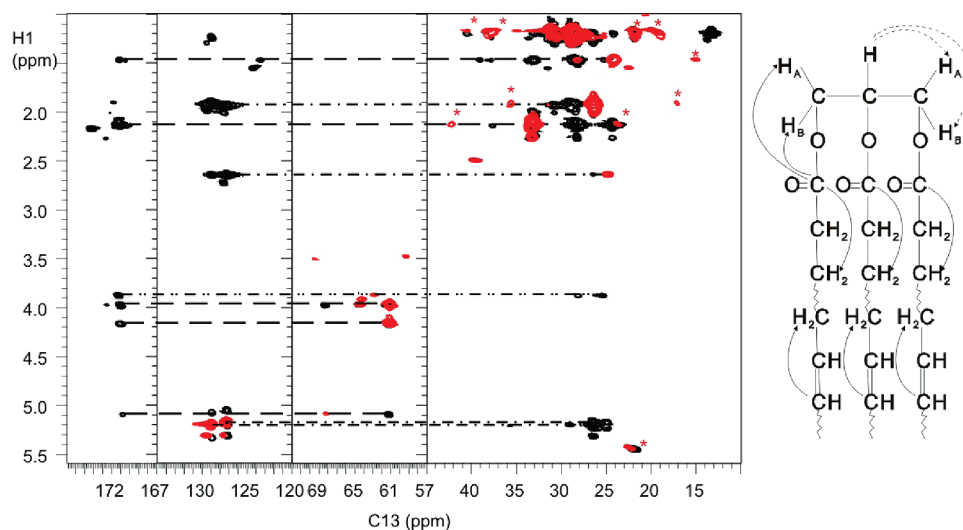


FIGURE 7: Overlaid sections of 2D HRMAS-gHMBC (black) and HRMAS-gHMQC (red) NMR spectra of melanin ghosts derived from 1:1 D-glucose and 1-<sup>13</sup>C-D-mannose, showing connectivities for triglycerides (---), unsaturated alkyl chains (- · -) and the alkoxy group of aliphatic ester chains(- · · -). The first and the third groups are connected to their respective carboxyl groups, whereas the unsaturated chains show connectivity between alkene and alkyl groups. The spectra were acquired with delay times corresponding to  $^1J_{CH} = 140$  Hz and  $^nJ_{CH} = 8$  Hz. The sample was spun at 2800 Hz at the magic angle. Positions of spinning sidebands are denoted by red (\*), 1400 Hz from the main peaks in the F1 (<sup>13</sup>C) dimension, 2800 Hz from the centerbands in the F2 (<sup>1</sup>H) dimension. COSY and HMBC connectivities that implicate a triglyceride structure are indicated by dashed and solid (H → C) curves, respectively. Monounsaturated chains are shown solely to illustrate alkene-alkane bonds but have not been demonstrated directly in this triglyceride.

a polysaccharide or protein, though more direct evidence is needed to verify this hypothesis.

*Identification of Glycerol Ester Structures in 1-<sup>13</sup>C-Mannose Melanin Ghost Samples.* It is tempting to attribute the prominent HRMAS-HMQC cross-peaks at (61, 3.97 ppm) and (61, 4.16 ppm) to C<sub>6</sub> of a sugar-based structure, but as compared with the isotopically enriched C-1 cross-peak at (101.8, 4.48 ppm), mannose-derived signals from

other sites are unlikely to be discernible at natural-abundance <sup>13</sup>C levels. Moreover, the spin connectivities observed in the 1-<sup>13</sup>C-mannose melanin sample do not support the presence of a sugar ring. Rather, <sup>1</sup>H-<sup>1</sup>H gmqCOSY measurements on DMSO-swelled samples (available as Supporting Information) reveal a *J*-coupled network among the protons resonating at 3.97, 4.16, and 5.09 ppm that is isolated from the upfield aliphatic protons. The respective <sup>13</sup>C shifts

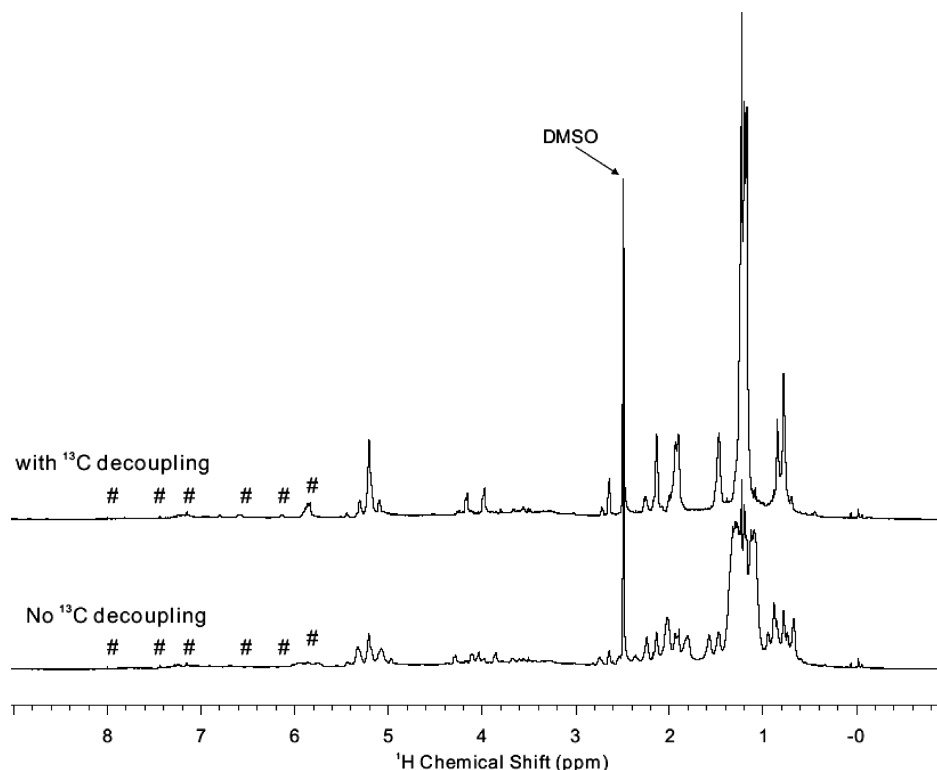


FIGURE 8: 600 MHz  $^1\text{H}$  HRMAS spectra of melanin ghosts derived from natural-abundance L-dopa and U- $^{13}\text{C}_6$ -glucose. The melanin sample was swollen in DMSO- $d_6$ , the spinning speed was 2.800 kHz, and the temperature was 50 °C. Positions of spinning sidebands are designated by (#).

observed in the HMQC spectrum of Figure 6 are 61, 61, and 68 ppm, implicating  $\text{CH}_n\text{O}$  structures and a pair of inequivalent protons at 3.97 and 4.16 ppm that are bound to the same carbon resonating at 61 ppm. This covalent connectivity information is confirmed by a comparison of HRMAS-HMQC and HRMAS-HMQC-TOCSY spectra (available as Supporting Information), which identifies the  $J$ -coupled proton network of each bound  $^{13}\text{C}$ - $^1\text{H}$  pair. Finally,  $^1\text{H}$ - $^{13}\text{C}$  HRMAS-HMBC experiments (Figure 7) link the  $\text{CH}_n\text{O}$  protons via long-range interactions to ester carboxyl groups: cross-peaks are evident at (170.9, 3.97), (170.9, 4.16) and (170.7, 5.09) ppm, respectively. HMBC data also link the carboxyl groups to  $^1\text{H}$  nuclei of the aliphatic chains (1.5 and 2.2 ppm). Taken together, these NMR chemical shifts and through-bond connectivities implicate a triglyceride structure as shown. The finding of triglycerides in melanin “ghosts” was unexpected given the harsh protocol used to isolate melanin. However, lipid vesicles have recently been reported in the *C. neoformans* cell wall (38), so it is possible that the highly reactive L-dopa oxidation intermediates react with triglycerides or that some of this material remains trapped within the melanin layers observed in ghost particles (13).

Also of note in Figure 7 are two HMBC cross-peaks that link vinyl and methylene groups (e.g., 127.2 with 5.21 and 2.63 ppm). Additionally, COSY and HMQC-TOCSY spectra (available as Supporting Information) show that a pair of vinyl CH resonances (at 127.2, 129.0, and 5.2 ppm) are linked with proton resonances at 2.63 and 1.91 ppm. Therefore, the alkyl chains must have one or more sites of unsaturation. Finally, an additional aliphatic carboxylate is implicated by an HMBC cross-peak at (171.2, 3.88 ppm) and an HMQC cross-peak at (62.8, 3.88 ppm). Although a triglyceride structure has been drawn to illustrate these

through-bond connectivities, it should be emphasized that the NMR data do not directly establish attachment of the glycerol and chain moieties.

*Incorporation of Glucose into Melanizing C. neoformans Cells.* A possible clue to the origin of the triglyceride and other aliphatic structures comes from biosynthetic incorporation experiments with U- $^{13}\text{C}_6$ -D-glucose, which is found to suffer a rather different metabolic fate than mannose. The  $^{13}\text{C}$  CPMAS spectra of Figure 4 display significant changes in both chemical shift and signal intensity for nearly all enriched carbons, suggesting the possibility of incorporation within  $(\text{CH}_2)_n$  (20–40 ppm),  $\text{CH}_n\text{O}$  (60–80), and  $\text{C}=\text{C}$  (129 ppm) groups of the melanized ghosts. That hypothesis is confirmed by the  $^1\text{H}$  HRMAS spectra of Figure 8, which show collapse of  $^1\text{H}$ - $^{13}\text{C}$  doublets in chain methylene, sugar, and double bond regions of the NMR spectrum upon  $^{13}\text{C}$  decoupling. Thus not surprisingly, glucose may be metabolized through various enzymatic pathways to yield numerous labeled products used in cell wall biosynthesis, or it may be used intact with its  $^{13}\text{C}$  labels as a major constituent of the polysaccharide cell walls (39). U- $^{13}\text{C}_6$ -glucose may also be the source of the aliphatic moieties present in *C. neoformans* melanin ghosts, either when present as the sole sugar source (as confirmed in Figure 8, and under further investigation) or possibly when mannose and glucose are both supplied in the growth media. As noted for 1- $^{13}\text{C}$ -D-mannose melanin, however, only those polysaccharides or triglycerides that are covalently bound to the melanin polymer are likely to survive the enzymatic and acid treatments used to generate the ghosts.

## CONCLUSIONS

CPMAS and HRMAS NMR methods, particularly when used in conjunction with introduction of specific  $^{13}\text{C}$  labels,

are well suited to the investigation of molecular structure and biosynthesis of *C. neoformans* melanin, a pigment associated with fungal virulence that has proved intractable for structural studies. *C. neoformans* provides a unique system for the study of melanogenesis and melanin assembly into cell walls because this fungus does not melanize unless provided with exogenous substrates for laccase-catalyzed melanin synthesis. Using 2,3-<sup>13</sup>C<sub>2</sub>-L-dopa and ring-<sup>13</sup>C<sub>6</sub>-L-dopa precursors, we demonstrated transformation of the L-dopa side chain to a proposed indole structure, obtaining results that reveal both the sites and structural modifications involved in polymer chain elongation and cross-linking within the *C. neoformans* melanin. Using a 1:1 mixture of glucose and 1-<sup>13</sup>C-mannose as sugar sources, it was shown that the mannose is present as a β-pyranose in the exhaustively purified melanin ghosts, suggesting direct incorporation of this sugar into fungal cell wall polysaccharides and the possibility of covalent binding to the pigment. However, U-<sup>13</sup>C<sub>6</sub>-D-glucose is broken down and incorporated into both polysaccharide cell walls and aliphatic chains that may be bound to the melanin. The aliphatic groups have been identified tentatively as triglyceride structures with one or more sites of chain unsaturation, which could serve in a chaperoning role for the hydrophobic melanin biopolymer.

Our ability to uncover these essential clues to the biosynthesis and ultimate molecular structure of *C. neoformans* melanin lays the groundwork for future targeting of the melanization pathway in therapeutic applications. The presence of polysaccharides, triglycerides, and indole-based melanin implies that the reactive intermediates posited by the Mason–Raper pathway for oxidation of L-dopa may react with nearby molecular moieties to form covalent links between the nascent melanin particle and cell wall structures. The resulting bonds could serve to attach melanin particles to the fungal cell walls, thus accounting for their enhanced structural robustness.

## ACKNOWLEDGMENT

Dr. Boris Itin provided essential assistance with the setup of high-field NMR experiments; Dr. Eriks Kupče provided expert advice regarding the use of adiabatic mixing in the HRMAS-assisted HMQC-TOCSY experiments; Prof. Steven Greenbaum permitted generous access to his EPR spectrometer at Hunter College; Dr. Javier Garcia-Rivera assisted with preparation of the melanin ghosts; Dr. Bingwu Yu provided the <sup>15</sup>N NMR spectrum of L-dopa melanin; Dr. Darón Freedberg offered essential critical feedback on carbohydrate NMR during the course of this work.

## SUPPORTING INFORMATION AVAILABLE

EPR spectrum of 2,3-<sup>13</sup>C-L-Dopa + U-<sup>13</sup>C<sub>6</sub>-D-glucose melanin (Figure S1); CPMAS <sup>15</sup>N NMR spectrum of ring-<sup>13</sup>C<sub>6</sub>-L-dopa + U-<sup>13</sup>C<sub>6</sub>-D-glucose melanin (Figure S2); HRMAS gHMQC-TOCSY and gmqCOSY comparison of 1-<sup>13</sup>C mannose melanin swelled in DMSO (Figure S3); HRMAS-HMQC and HMQC-TOCSY comparison of 1-<sup>13</sup>C mannose melanin swelled in DMSO (Figure S4). This material is available free of charge via the Internet at <http://pubs.acs.org>.

## REFERENCES

- Hill, H. Z. (1992) The function of melanin or six blind people examine an elephant. *BioEssays* 14, 49–56.
- Adhyaru, B. B., Akhmedov, N. G., Katritzky, A. R., and Bowers, C. R. (2003) Solid-state cross-polarization magic angle spinning <sup>13</sup>C and <sup>15</sup>N NMR characterization of Sepia melanin, Sepia melanin free acid and Human hair melanin in comparison with several model compounds. *Magn. Reson. Chem.* 41, 466–474.
- Schwabe, K., Lassman, G., Damerau, W., and Naundorf, H. J. (1989) Protection of melanoma cells against superoxide radicals by melanins. *Cancer Res. Clin. Oncol.* 115, 597–600.
- Kinnaert, E., Morandini, R., Simon, S., Hill, H. Z., Ghanem, G., and Van Houtte, P. (2000) The degree of pigmentation modulates the radiosensitivity of human melanoma cells. *Radiat. Res.* 154, 497–502.
- Jacobson, E. S. (2000) Pathogenic roles for fungal melanins. *Clin. Microbiol. Rev.* 13, 708.
- Henson, J. M., Butler, M. J., and Day, A. W. (1999) The dark side of the mycelium: melanins of phytopathogenic fungi. *Annu. Rev. Phytopathol.* 37, 447–471.
- Schnitzer, M., and Chan, Y. K. (1986) Structural characteristics of a fungal melanin and soil humic acid. *Soil Sci. Soc. Am. J.* 50, 67–71.
- Duff, G. A., Roberts, J. E., and Foster, N. (1988) Analysis of the structure of synthetic and natural melanins by solid-phase NMR. *Biochemistry* 27, 7112–7116.
- Herve, M., Hirschinger, J., Granger, P., Gilard, P., Deflandre, A., and Goetz, N. (1994) A <sup>13</sup>C solid-state NMR study of the structure and auto-oxidation process of natural and synthetic melanins. *Biochim. Biophys. Acta* 1204, 19–27.
- Knicker, H., Almendros, G., González-Vila, F. J., Lüdemann, H. D., and Martin, F. (1995) <sup>13</sup>C and <sup>15</sup>N NMR analysis of some fungal melanins in comparison with soil organic matter. *Org. Geochem.* 23, 1023–1028.
- Aime, S., Fasano, M., Bergamasco, B., Lopiano, L., and Quatrocchio, G. (1996) Nuclear Magnetic resonance spectroscopy characterization and iron content determination of human mesencephalic neuromelanin, in *Advances in Neurology*, pp 263–270, Lippincott-Raven Publishers, Philadelphia.
- Tian, S., Garcia-Rivera, J., Yan, B., Casadevall, A., and Stark, R. E. (2003) Unlocking the molecular structure of fungal melanin using <sup>13</sup>C biosynthetic labeling and solid-state NMR. *Biochemistry* 42, 8105–8109.
- Eisenman, H. C., Nosanchuk, J. D., Webber, J. B., Emerson, R. J., Camesano, T. A., and Casadevall, A. (2005) Microstructure of cell wall-associated melanin in the human pathogenic fungus *Cryptococcus neoformans*. *Biochemistry* 44, 3683–3693.
- Nosanchuk, J., and Casadevall, A. (2006) Impact of melanin on microbial virulence and clinical resistance to antimicrobial compounds. *Antimicrob. Agents Chemother.* 50, 3519–3528.
- Dadachova, E., and Casadevall, A. (2005) Melanin as a potential target for radionuclide therapy of metastatic melanoma. *Future Oncol.* 1, 541–549.
- Dadachova, E., Bryan, R. A., Huang, X., Moadel, T., Schweitzer, A. D., Nosanchuk, J. D., and Casadevall, A. (2007) Ionizing radiation changes the electronic properties of melanin and enhances the growth of melanized fungi. *PLoS ONE* 2, e457.
- Prota, G. (1992) *Melanins and Melanogenesis*, Academic Press, San Diego, CA.
- Williamson, P. R., Wakamatsu, K., and Ito, S. (1998) Melanin biosynthesis in *Cryptococcus neoformans*. *J. Bacteriol.* 180, 1570–1572.
- Rosas, A. L., Nosanchuk, J. D., Gómez, B. L., Edens, W. A., Henson, J. M., and Casadevall, A. (2000) Isolation and serological analyses of fungal melanins. *J. Immun. Methods* 244, 69–80.
- Dubois, M., Gilles, K. A., Rebers, P. A., Smith, F. (1956) Colorimetric method for determination of sugars and related substances. *Anal. Chem.* 28, 350–356.
- Bennett, A. E., Rienstra, C. M., Auger, M., Lakshmi, K. V., and Griffin, R. G. (1995) Heteronuclear decoupling in rotating solids. *J. Chem. Phys.* 103, 6951–6958.
- Hurd, R. E., and John, B. K. (1991) Gradient enhanced proton-detected heteronuclear multiple-quantum coherence spectroscopy. *J. Magn. Reson.* 91, 648–653.
- Rance, M., Sørensen, O. W., Bodenhausen, G., Wagner, G., Ernst, R. R., and Wüthrich, K. (1983) Improved spectral resolution in COSY <sup>1</sup>H NMR spectra of proteins via double quantum filtering. *Biochem. Biophys. Res. Commun.* 117, 479–485.
- Bax, A., and Morris, G. A. (1981) An improved method for heteronuclear chemical shift correlation by two-dimensional NMR. *J. Magn. Reson.* 42, 501–502.

25. Bax, A., and Summers, M. F. (1986)  $^1\text{H}$  and  $^{13}\text{C}$  assignments from sensitivity-enhanced detection of heteronuclear multiple-bond connectivity by 2D multiple quantum NMR. *J. Am. Chem. Soc.* **108**, 2093–2094.
26. Rinaldi, P. L., and Keifer, P. A. (1994) The utility of pulsed-field-gradient HMBC for organic structure determination. *J. Magn. Reson. A* **108**, 259–262.
27. Shaka, A. J., Barker, P. B., and Freeman, R. (1985) Computer-optimized decoupling scheme for wideband applications and low-level operation. *J. Magn. Reson.* **64**, 547–552.
28. Kupče, E., and Hiller, W. (2001) Clean adiabatic TOCSYs. *Magn. Reson. Chem.* **39**, 231–235.
29. Subianto, S., Will, G., and Meredith, P. (2005) Electrochemical synthesis of melanin free-standing films. *Polymer* **46**, 11505–11509.
30. Tran, M. L., Powell, B. J., and Meredith, P. (2006) Chemical and structural disorder in eumelanins: a possible explanation for broadband absorbance. *Biophys. J.* **90**, 743–752.
31. Garcia-Rivera, J., Eisenman, H. C., Nosanchuk, J. D., Aisen, P., Zaragoza, O., Moadel, T., Dadachova, E., and Casadevall, A. (2005) Comparative analysis of *Cryptococcus neoformans* acid-resistant particles generated from pigmented cells grown in different laccase substrates. *Fungal Genet. Biol.* **42**, 989–998.
32. Aime, S., Fasano, M., Terreno, E., and Groombridge, C. J. (1991) NMR Studies of Melanins: characterization of a soluble melanin free acid from *Sepia* ink. *Pigm. Cell Res.* **4**, 216–221.
33. Cherniak, R., O'Neill, E. B., and Sheng, S. (1998) Assimilation of xylose, mannose, and mannitol for synthesis of glucuronoxylomannan of *Cryptococcus neoformans* determined by  $^{13}\text{C}$  nuclear magnetic resonance spectroscopy. *Infect. Immun.* **66**, 2996–2998.
34. Zhu, Y., Zajicek, J., and Serianni, A. S. (2001) Acyclic forms of [ $1\text{-}^{13}\text{C}$ ]Aldohexoses in aqueous solution: Quantitation by  $^{13}\text{C}$  NMR and deuterium isotope effects on tautomeric equilibria. *J. Org. Chem.* **66**, 6244–6251.
35. Lindberg, J. J., and Hortling, B. (1985) Cross polarization-magic angle spinning NMR studies of carbohydrates and aromatic polymers. *Adv. Polym. Sci.* **66**, 1–22.
36. Reiss, E., White, E. H., Cherniak, R., and Dix, J. E. (1986) Ultrastructure of acapsular mutant *Cryptococcus neoformans* cap 67 and monosaccharide composition of cell extracts. *Mycopathologia* **93**, 45–54.
37. Vartivarian, S. E., Reyes, G. H., Jacobson, E. S., James, P. G., Cherniak, R., Mumaw, V. R., and Tingler, M. J. (1989) Localization of mannoprotein in *Cryptococcus neoformans*. *J. Bacteriol.* **171**, 6850–6852.
38. Rodrigues, M. L., Nimrichter, L., Oliveira, D. L., Frases, S., Miranda, K., Zaragoza, O., Alvarez, M., Nakouzi, A., Feldmesser, M., and Casadevall, A. (2007) Vesicular polysaccharide export in *Cryptococcus neoformans* is a eukaryotic solution to the problem of fungal trans-cell wall transport. *Eukaryot. Cell* **6**, 48–59.
39. Casadevall, A., and Perfect, J. R. (1998) *Cryptococcus neoformans*. ASM Press, Herndon, VA.

BI702093R